

# Electronic and Structural Properties of a 4d-Perovskite: Cubic Phase of SrZrO<sub>3</sub>

E. Mete, R. Shaltaf, and Ş. Ellialtıođlu\*

*Department of Physics, Middle East Technical University, Ankara 06531, Turkey*

(Dated: October 24, 2018)

First-principles density functional calculations are performed within the local density approximation to study the electronic properties of SrZrO<sub>3</sub>, an insulating 4d-perovskite, in its high-temperature cubic phase, above 1400 K, as well as the generic 3d-perovskite SrTiO<sub>3</sub>, which is also a  $d^0$ -insulator and cubic above 105 K, for comparison reasons. The energy bands, density of states and charge density distributions are obtained and a detailed comparison between their band structures is presented. The results are discussed also in terms of the existing data in the literature for both oxides.

PACS numbers: 71.15.Mb, 71.20.-b

## I. INTRODUCTION

The class of transition metal oxides constitutes a big family of interesting materials with extra physical properties due to the additional d-electrons they possess. They come in variety of crystal structures and exhibit individually several of these phases. They include insulators, metals, semiconductors and also superconductors. Some have delocalized d-bands providing catalytically active surfaces, some have narrow d-bands with emphasized electron correlations giving rise to diverse properties like high temperature superconductivity, and colossal magnetoresistance. They are well known with their ferroelectric, antiferroelectric and piezoelectric properties. Their use in technological application is also diverse, including optical wave guides, laser-host crystals, high temperature oxygen sensors, surface acoustic wave devices, non-volatile memories, dynamic random access memories, frequency doublers, piezoelectric actuator materials, and high-K capacitors in various applications.

Strontium titanate, SrTiO<sub>3</sub>, is a generic representative of transition metal oxides which have perovskite crystalline structure. It has been extensively studied both theoretically and experimentally because of its several interesting physical and technological properties. It is highly insulating at room temperature, and in the form of n-type thin films it shows superconductivity at low temperatures. It is a cubic perovskite at room temperature with a tetragonal phase transition at 105 K. Its surfaces are very flat and stable both mechanically and chemically which makes it best electrode in photocatalysis of water<sup>1</sup>, and makes it best buffer layer for the growth of gallium arsenide on silicon<sup>2</sup>, and makes it best substrate for the growth of high T<sub>c</sub> cuprate superconductors<sup>3</sup>. Due to its high dielectric constant it is also one of the leading candidates to replace the silica as a gate material in silicon technology.

Another insulating perovskite is the strontium zir-

conate, SrZrO<sub>3</sub>, with 4d-electrons, which is of interest because of its high temperature electronic properties. Large single crystals of SrZrO<sub>3</sub> with high perfection can be grown with recent techniques and this enables their usage as laser-host materials and as substrate materials. It was also suggested by Shende *et al.*<sup>4</sup> that these materials can be used in high-voltage capacitor applications because of their high breakdown strengths as well as high dielectric constant. In addition to this, both SrTiO<sub>3</sub> and SrZrO<sub>3</sub> are suitable for use in high-temperature applications such as fuel cells, steam electrolysis and hydrogen gas sensors<sup>5,6,7</sup>. This is because when these type of transition metal oxides are doped with acceptor ions they exhibit protonic conduction at high temperatures<sup>8</sup>.

Unlike SrTiO<sub>3</sub>, at room temperature SrZrO<sub>3</sub> has an orthorhombic phase as revealed by the first structural studies which date back to 1960's<sup>9,10</sup>. Later the existence of two additional phases at high-temperature was proposed by Carlsson to be both tetragonal<sup>11</sup>, however, more recent studies<sup>12,13,14</sup> on high temperatures have shown that SrZrO<sub>3</sub> undergoes three structural phase transitions summarized as follows: First, orthorhombic ( $Pnma$ ) to orthorhombic ( $Cmcm$ ) at 970 K, then to tetragonal ( $I4/mcm$ ) at 1100 K, and then to cubic ( $Pm3m$ ) at 1400 K. This compound has a rather high melting temperature of about 2920 K<sup>15</sup>, consequently it is cubic in a wide range of temperature where most of its useful applications take place.

In this work we have made first-principles pseudopotential calculations of the electronic band structure, density of states and charge densities for SrZrO<sub>3</sub> in the cubic perovskite phase. In addition to that we have made a reference calculation for SrTiO<sub>3</sub> in order to give a discussion by comparison. We have also made some comparisons with the related experimental data where available.

## II. CALCULATION METHOD

We used pseudopotential method based on density functional theory in the local density approximation (LDA). The self consistent norm conserving pseudopotentials are generated by using the Troullier-Martins

---

\*Corresponding author. E-mail: sinasi@metu.edu.tr

scheme<sup>16</sup> which is included in the fhi98PP package<sup>17</sup>. Plane waves are used as a basis set for the electronic wave functions. In order to solve the Kohn-Sham equations<sup>18</sup>, conjugate gradients minimization method<sup>19</sup> is employed as implemented by the ABINIT code<sup>20</sup>. The exchange-correlation effects are taken into account within the Perdew-Wang scheme<sup>21</sup> as parameterized by Ceperly and Alder<sup>22</sup>.

Pseudopotentials are generated using the following electronic configurations: For Sr 5s electrons are considered as the true valence. Moreover the 4s and 4p semicore states are added to the valence states. For O only the true valence states (2s and 2p) are taken into account, because these states are enough to have the correct transferability property. For Ti 4s and 3d true valence states plus the 3s and 3p semicore states are treated as valence states. Similarly, for the same group element Zr, 5s and 4d true states and additionally the 4s and 4p semicore states are considered as valence states. Inclusion of semicore states in the case of Sr, Ti and Zr is required in order to get the correct electronic properties of these elements in various physical systems. In other words, the inclusion of these semicore states make the corresponding pseudopotentials closer to the all-electron potentials. The above configuration is found to be the optimized choice for these materials.

All of the calculations involve 5-atom cubic unit cell arranged in a perovskite structure. We get a good convergence for the bulk total energy calculation with the choice of cut-off energies at 30 Ha for SrTiO<sub>3</sub> and at 33 Ha for SrZrO<sub>3</sub> using  $4 \times 4 \times 4$  Monkhorst-Pack<sup>23</sup> mesh grid. We have found that in the band structure calculations 76 **k**-points are enough to obtain good results for both of these transition metal oxides. In the density of states calculations, however, the irreducible Brillouin zone was sampled with 560 and 455 **k**-points for SrTiO<sub>3</sub> and SrZrO<sub>3</sub>, respectively.

### III. RESULTS AND DISCUSSION

The results for structural parameter calculations are summarized in Table I. The calculated lattice parameters for SrTiO<sub>3</sub> and SrZrO<sub>3</sub> are both within 0.5% of the experimental results. Likewise the calculated bulk moduli for SrTiO<sub>3</sub> and SrZrO<sub>3</sub> are found to be 0.3% and 0.8% smaller than the effective experimental values, respectively. The agreement with the experiments can be considered to be very good. In the case of SrTiO<sub>3</sub>, comparisons of our results with the theoretical work of Kimura *et al.*<sup>24</sup> and with the calculated values of van Benthem *et al.*<sup>25</sup> suggest that our pseudopotentials are as reliable and perform slightly better. To our knowledge no first-principles calculation is available for SrZrO<sub>3</sub> to compare with.

For the bulk modulus of SrZrO<sub>3</sub>, we have listed in Table I an extrapolated value of 150 GPa by Ligny and Richet<sup>12</sup>, however, such extrapolation is known to give

about 15% underestimation for the **Zr**-compound in a series of CaMO<sub>3</sub><sup>26</sup>, and by the same token we expect the experimental value to be higher than 150 GPa.

	Lattice Parameter (Å)		Bulk Modulus (GPa)	
	Calc.	Exp.	Calc.	Exp.
SrTiO <sub>3</sub>	3.878	3.905 <sup>27</sup>	191	183 <sup>27</sup>
SrZrO <sub>3</sub>	4.095	4.109 <sup>28</sup>	171	150 <sup>12</sup>

TABLE I: Calculated and experimental values for lattice parameter and bulk modulus of SrTiO<sub>3</sub> and SrZrO<sub>3</sub>

Energy band structures and densities of states are given in Fig. 1, where the zero of energy is chosen to coincide with the top of the valence band. The general features of the energy bands are similar for both oxides. An overall look at the two band structures shows that the lower valence bands are composed of O 2s and Sr 4p semicore states grouped together at about -15 eV. Although the individual bands have similar bandwidths for both materials, those of SrTiO<sub>3</sub> do not overlap and separated by a  $\sim 1$  eV gap, whereas those of SrZrO<sub>3</sub> having stronger interaction with each other, especially around X point, causing an overlap of the corresponding densities of states, and consequently, the combined bandwidth is smaller.

The upper valence bands have the same trend, i.e., wider for SrTiO<sub>3</sub> (4.93 eV) and narrower for SrZrO<sub>3</sub> (4.32 eV). Top of the valence bands reflect the *p* electronic character mostly due to oxygen-oxygen interaction (down to about -4 eV) for both of the transition metal oxides. This agrees well with the DV-X $\alpha$  molecular orbital study of Yoshino *et al.*<sup>29</sup>. Even though whole valence band structure is dominated by O 2p states, there are, however, a mixture of  $\sigma$ -bands stemming from the *pd* $\sigma$  interactions extending throughout the whole valence band width, and  $\pi$ -bands due to *pd* $\pi$  interactions which are narrower than that.

Both of SrTiO<sub>3</sub> and SrZrO<sub>3</sub> have their valence band maxima at the R point. The energy values of the uppermost band at  $\Gamma$  and M points lie slightly lower than its value at the point R. In SrTiO<sub>3</sub> bottom of the valence band occurs at R, whereas in SrZrO<sub>3</sub> it occurs at M point. In both cases, however, these energy eigenvalues are close to each other at M and R points with a difference, larger one being for the SrZrO<sub>3</sub>, of only 0.25 eV.

The lower conduction bands are mainly Ti 3d or Zr 4d states hybridized with some O 2p electrons giving rise to antibonding  $\pi^*$ - and  $\sigma^*$ -bands. In the case of SrTiO<sub>3</sub> the conduction band ordering is as follows: Ti 3d  $t_{2g}$  ( $\pi^*$ -triplet) bands stand alone next to the gap with no overlap to the Ti 3d  $e_g$  states ( $\sigma^*$ -doublet) which lie just above, and upper parts of which are mixed with the lower extension of Sr 5s and 4d  $t_{2g}$  bands. This ordering is slightly different for SrZrO<sub>3</sub>, especially at high energies. Zr 4d  $t_{2g}$  states are next to the gap and their upper parts are mixed with Sr 5s and 4d  $t_{2g}$  states. Zr 4d  $e_g$  states lie further up

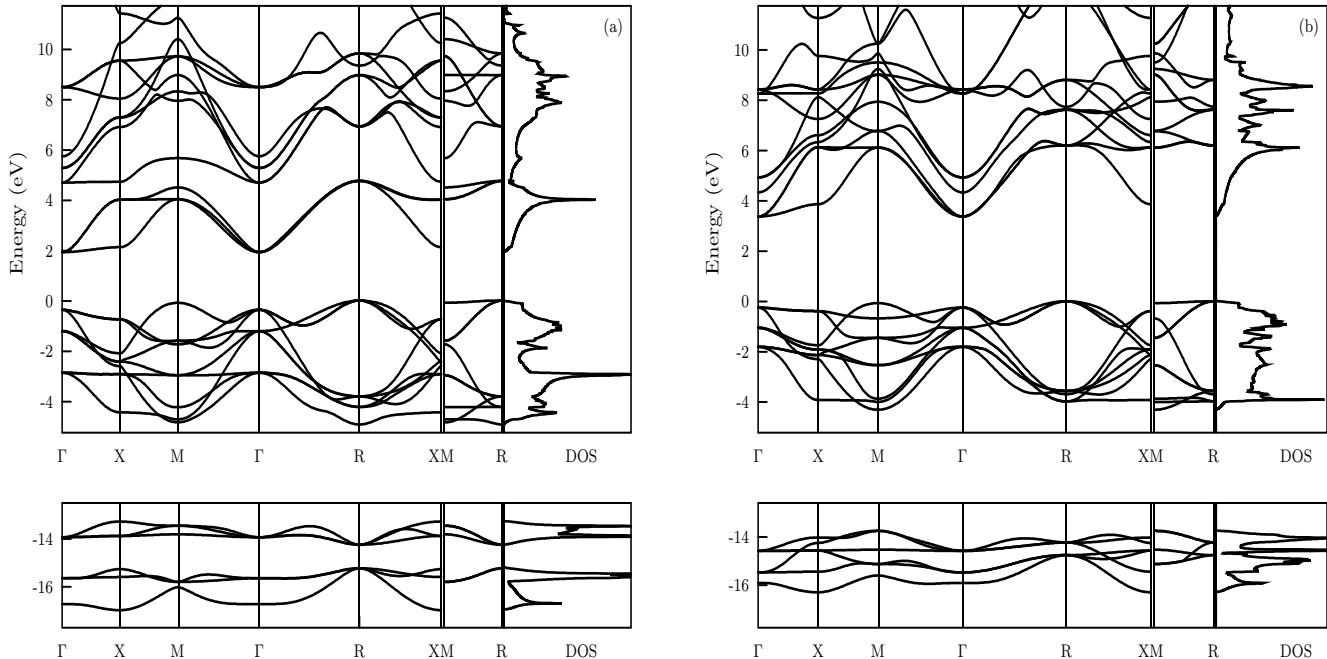


FIG. 1: Calculated band structures for (a) SrTiO<sub>3</sub> and (b) SrZrO<sub>3</sub>

in the energy region between 8.1 eV and 12.5 eV. Conduction band minimum occurs at  $\Gamma$  point in both materials. The lowest conduction band along  $\Gamma X$  is more dispersed in strontium zirconate, and consequently the conduction band edge of its density of states is of three dimensional nature. Calculated  $\pi^*$ -conduction band widths are 2.83 eV for SrTiO<sub>3</sub> and 3.39 eV for SrZrO<sub>3</sub>.

For SrTiO<sub>3</sub> the calculated indirect energy band gap between  $\Gamma$  and R points is found to be 1.92 eV and the direct band gap is 2.30 eV. Corresponding experimental values are 3.25 eV and 3.75 eV<sup>25</sup>, respectively. The results obtained for SrZrO<sub>3</sub> are on the other hand as follows: Indirect band gap is 3.37 eV between  $\Gamma$  and R points. The direct band gap being 3.62 eV, is again smaller than the experimental value of 5.9 eV<sup>30</sup>. This disagreement between the calculations and experimental values resulting in narrower theoretical band gaps is a well known artifact<sup>31</sup> of LDA and does not have any significant effect on the rest of the band structure.

Looking at the density of states pictures one observes several structures common to both materials. Most of these correspond to singularities in the bands. There are three flat bands in the conduction band of both materials. Lowest one is Ti (Zr)  $t_{2g}$  band along XM at about 4 eV (6 eV) which causes the well defined  $\pi^*$  peak with a logarithmic van Hove singularity in the density of states characteristic of two dimensionality of these bands. The next one up is the Ti (Zr)  $e_g$  band along  $\Gamma X$  at 4.68 eV (8.24 eV) causing a jump discontinuity in the density of states. Similar  $\sigma^*$  shoulder in density of states is caused by the third flat band which is again Ti (Zr)  $e_g$  band

along MR at about 9 eV (12.5 eV, not shown).

Valence bands are slightly different in terms of van Hove singularities. SrTiO<sub>3</sub> has a very significant flat band at -2.87 eV along  $\Gamma X M \Gamma$  which is a non-bonding  $\sigma_0$  band due to O  $2p$  and responsible for the highest peak at the center of the valence band. Ti  $3d t_{2g}$  band at the same energy along  $\Gamma X$  is rather flat, and at about -4.5 eV along XM and also RX it is quite flat close to the X-side. In addition, the band at -4.25 eV along MR looks almost flat but the corresponding density of states shows three dimensional behavior just slightly. For the SrZrO<sub>3</sub> valence band, at about -4 eV, the Zr  $t_{2g}$  state along XM, MR and RX are the only flat bands causing the highest peak located at the bottom of the valence band. The band corresponding to the oxygen non-bonding state located at the center of SrTiO<sub>3</sub> valence band density of states is dispersed in all directions for SrZrO<sub>3</sub>.

Charge density plots were obtained for the lowest three conduction bands degenerate at the  $\Gamma$  point for a (001) plane containing the transition metal and the four neighboring oxygens. Fig. 2 shows the composition of these bands to be clearly the hybridization between transition metal  $d$ -orbitals with  $t_{2g}$  symmetry and O  $2p$  orbitals. The corresponding  $\pi^*$  bands shown in Fig. 1 are more singled out for SrTiO<sub>3</sub> and consequently the charge is more localized as compared to SrZrO<sub>3</sub> whose  $\pi^*$  bands are not separated from the rest of the conduction bands.

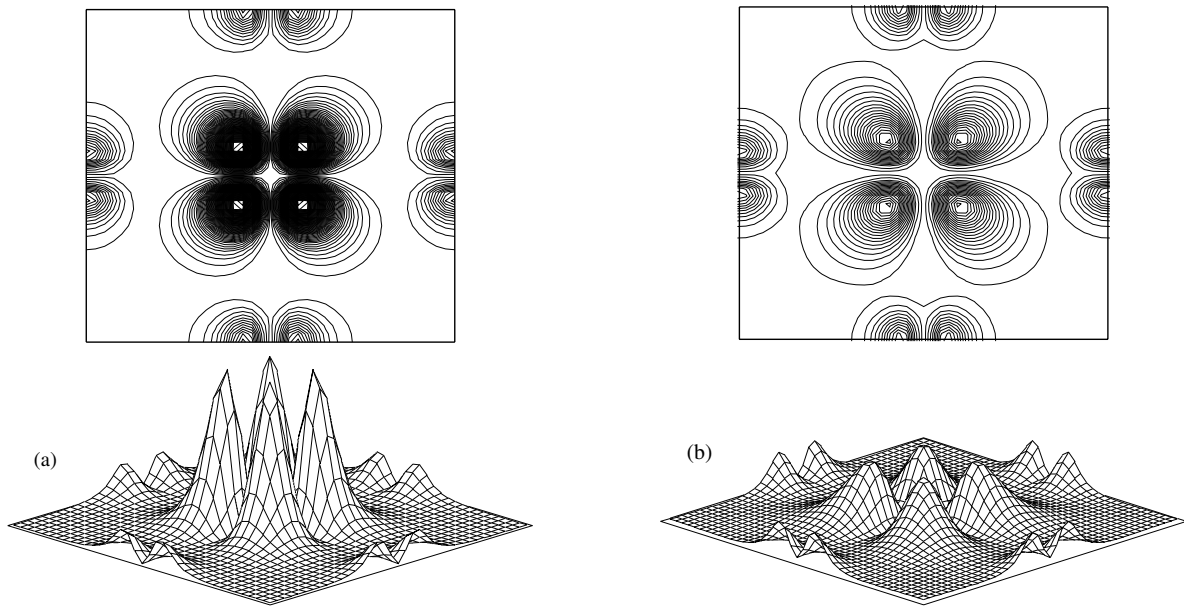


FIG. 2: Charge density contour plots for  $\pi^*$  bands for (a) SrTiO<sub>3</sub> and (b) SrZrO<sub>3</sub>

#### IV. CONCLUSION

The structural and electronic properties of two  $d^0$ -insulator metal oxides, SrZrO<sub>3</sub> and SrTiO<sub>3</sub>, with cubic perovskite structure are studied using an ab-initio pseudopotential method. Structural parameters are found to compare well with the available data in the literature. A detailed description of their energy bands are given. Corresponding density of states are presented and the major structures in them are identified. Charge density functions are displayed for the lower conduction bands for both oxides. Our results for the electronic properties

of SrTiO<sub>3</sub> are shown to agree with other calculations and experimental findings whereas those of SrZrO<sub>3</sub> are compared only with the estimations of Lee *et al.*<sup>30</sup> from their optical conductivity spectra, since to our knowledge, no theoretical calculations exist in the literature.

#### V. ACKNOWLEDGEMENT

This work was supported by TÜBİTAK, The Scientific and Technical Research Council of Turkey, Grants No. TBAG-2036 (101T058).

- 
- <sup>1</sup> Natasha Erdman, Kenneth R. Poeppelmeier, Mark Asta, Oliver Warshkow, Donald E. Ellis, and Laurence D. Marks, *Nature* **419**, 55 (2002).
  - <sup>2</sup> R. Droopard, Z. Yu, J. Ramdani, L. Hilt, J. Curless, C. Overgaard, J.L. Edwards Jr., J. Finder, K Eisenbeiser, W. Ooms, *Mater. Sci. Eng. B* **87**, 292 (2001).
  - <sup>3</sup> C. Aruta, *Phys. Stat. Sol. (a)* **183**, 353 (2001).
  - <sup>4</sup> Rajesh V. Shende, Daniel S. Krueger, George A. Rosetti Jr., and Stephen J. Lombardo, *J. Am. Ceram. Soc.* **84**, 1648 (2001).
  - <sup>5</sup> H. Iwahara, T. Yajima, T. Hibino, and H. Ushida, *J. Electrochem. Soc.* **140**, 1687 (1993).
  - <sup>6</sup> N. Kurita, N. Fukatsu, and T. Ohashi, *J. Jpn. Inst. Metals* **58**, 782 (1994).
  - <sup>7</sup> T. Yajima, K. Koide, H. Takai, N. Fukatsu, and H. Iwahara, *Solid State Ionics* **79**, 333 (1995).
  - <sup>8</sup> H. Iwahara, T. Esaka, H. Uchida, and N. Maeda, *Solid State Ionics* **3/4**, 359 (1981).
  - <sup>9</sup> R. S. Roth, *J. Res. Natl. Bur. Stand.* **58**, 75 (1957).
  - <sup>10</sup> H. E. Swanson, M. I. Cook, T. Isaacs, and E. H. Evans, *Natl. Bur. Stand. Circ.* **539**, 51 (1960).
  - <sup>11</sup> L. Carlsson, *Acta Cryst.* **23**, 901 (1967), *J. Mater. Csi.* **5**, 325 (1970).
  - <sup>12</sup> Dominique de Ligny and Pascal Richet, *Phys. Rev. B* **53**, 3013 (1996).
  - <sup>13</sup> J. Kennedy Brendan, Christopher J. Howard, and Bryan C. Chakoumakos, *Phys. Rev. B* **59**, 4023 (1999).
  - <sup>14</sup> Tetsushi Matsuda, Shiisuke Yamakama, Ken Kurosaki, and Shin-ichi Kobayashi, *J. Alloys Comp.* **351**, 43 (2003).
  - <sup>15</sup> D. Souptel, G. Behr, and A. M. Balbashov, *J. Cryst. Gro.* **236**, 583 (2002).
  - <sup>16</sup> N. Troullier and J. L. Martins, *Phys. Rev. B* **43**, 1993 (1991).
  - <sup>17</sup> Martin Fuchs and Mathias Scheffler, *Comp. Phys. Commun.* **119**, 67 (1999).
  - <sup>18</sup> W. Kohn and L. J. Sham, *Phys. Rev.* **140**, 1133A (1965).
  - <sup>19</sup> M.C. Payne, M.P. Teter, D.C. Allan, T.A. Arias and J.D. Joannopoulos, *Rev. Mod. Phys.* **64**, 1045 (1992).
  - <sup>20</sup> X. Gonze, J.-M. Beuken, R. Caracas, F. Detraux, M.

- Fuchs, G.-M. Rignanese, L. Sindic, M. Verstraete, G. Zerah, F. Jollet, M. Torrent, A. Roy, M. Mikami, Ph. Ghosez, J.-Y. Raty, and D. C. Allan. *Comp. Mater. Sci.* **25**, 478 (2002).
- <sup>21</sup> J. P. Perdew and Y. Wang, *Phys. Rev. B* **45**, 13244 (1992).
- <sup>22</sup> D. M. Ceperly and B. J. Alder, *Phys. Rev. Lett.* **45**, 566 (1980).
- <sup>23</sup> H. J. Monkhorst, and J. D. Pack, *Phys. Rev. B* **13**, 5188 (1976).
- <sup>24</sup> S. Kimura, J. Yamauchi, M. Tsukada, and S. Watanebe, *Phys. Rev. B* **51** 11049 (1995).
- <sup>25</sup> K. van Benthem, C. Elsässer, and R. H. French, *J. Appl. Phys.* **90**, 6156 (2001).
- <sup>26</sup> Nancy L. Ross, Ross J. Angel, Jennifer Kung, and Tracey D. Chaplin, *Mat. Res. Soc. Symp. Proc.* **718**, D2.4 (2002).
- <sup>27</sup> T. Mitsui and S. Nomura (eds.), “Numerical Data and Functional Relations in Science and Technology—Crystal and Solid State Physics”, (Landoldt-Börnstein, New Series, Group III, Vol **16**, Pt. a Springer-Verlag, Berlin, 1982)
- <sup>28</sup> A. J. Smith and A. J. E. Welch, *Acta Cryst.* **13**, 653 (1960).
- <sup>29</sup> M. Yoshino, K. Nakatsuka, H. Yukawa, and M. Morinaga, *Solid State Ionics* **127**, 109 (2000).
- <sup>30</sup> Y. S. Lee, J. S. Lee, T. W. Noh, D.Y. Byun, K. S. Yoo, K. Yamaura, and E. Takayama-Muromachi, *cond-mat/0207012*.
- <sup>31</sup> R. O. Jones and O. Gunnarsson, *Rev. Mod. Phys.* **61**,689 (1989).